

# Protein Export Marks the Early Phase of Gametocytogenesis of the Human Malaria Parasite *Plasmodium falciparum*\*

Francesco Silvestrini‡§, Edwin Lasonder§¶, Anna Olivieri‡, Grazia Camarda‡, Ben van Schaijk||, Massimo Sanchez\*\*, Sumera Younis Younis‡ ††, Robert Sauerwein||, and Pietro Alano‡§§

Despite over a century of study of malaria parasites, parts of the *Plasmodium falciparum* life cycle remain virtually unknown. One of these is the early gametocyte stage, a round shaped cell morphologically similar to an asexual trophozoite in which major cellular transformations ensure subsequent development of the elongated gametocyte. We developed a protocol to obtain for the first time highly purified preparations of early gametocytes using a transgenic line expressing a green fluorescent protein from the onset of gametocytogenesis. We determined the cellular proteome (1427 proteins) of this parasite stage by high accuracy tandem mass spectrometry and newly determined the proteomes of asexual trophozoites and mature gametocytes, identifying altogether 1090 previously undetected parasite proteins. Quantitative label-free comparative proteomics analysis determined enriched protein clusters for the three parasite developmental stages. Gene set enrichment analysis on the 251 proteins enriched in the early gametocyte proteome revealed that proteins putatively exported and involved in erythrocyte remodeling are the most overrepresented protein set in these stages. One-tenth of the early gametocyte-enriched proteome is constituted of putatively exported proteins, here named PfGEXPs (*P. falciparum* gametocyte-exported proteins). N-terminal processing and N-acetylation at a conserved leucine residue within the *Plasmodium* export element pentamotif were detected by mass spectrometry for three such proteins in the early but not in the mature gametocyte sample, further supporting a specific role in protein export in early gametocytogenesis. Previous reports and results of our experiments confirm that the three proteins are indeed exported in the

erythrocyte cytoplasm. This work indicates that protein export profoundly marks early sexual differentiation in *P. falciparum*, probably contributing to host cell remodeling in this phase of the life cycle, and that gametocyte-enriched molecules are recruited to modulate this process in gametocytogenesis. *Molecular & Cellular Proteomics* 9:1437–1448, 2010.

The burden imposed by malaria protozoan parasites to human populations worldwide is due to the severity of the disease, particularly when caused by the species *Plasmodium falciparum*, and to the efficient transmission of the parasite between humans and the *Anopheles* mosquito vectors. Gametocytes, the precursors of male and female gametes, are the *Plasmodium* developmental stages critical to the transmission of the parasites from the human blood stream to the mosquito gut when the insect bites an infected individual. In the human host and in *in vitro* cultures, *P. falciparum* gametocytogenesis proceeds in about 10 days through the five classically described morphological stages I to V (1). The typical elongated form of gametocytes in this species appears around day 2 of maturation in the crescent-shaped stage II gametocyte, which progressively further elongates during maturation. In *P. falciparum* infections, only mature stage V gametocytes are detectable in the peripheral circulation, whereas earlier stages are sequestered in internal organs (2).

Although malaria parasites were discovered over a century ago, knowledge on parts of the *Plasmodium* life cycle is still very poor. One such stage is the early stage I gametocyte, which is morphologically very similar to a pigmented asexual trophozoite. The molecular characterization of this stage was for long restricted to the identification of two abundant gametocyte-specific proteins, Pfs16 (PFD0310w) and Pfg27 (PF13\_0011), up-regulated, respectively, from 24 and 30 h postinvasion (3, 4). Recently, transcriptome analyses comparing isogenic parasites able and unable to produce gametocytes identified genes up-regulated at the onset of gametocytogenesis (5, 6) and characterized four gametocyte-specific proteins significantly up-regulated in the first 30–40 h of sexual differentiation, Pfmdv-1/peg3 (PFL0795c) (5, 7), Pfpeg4 (PF10\_0164) (5), and Pfg14.744 and Pfg14.748 (PF14\_0744

From the ‡Dipartimento di Malattie Infettive, Parassitarie e Immunomediate, Istituto Superiore di Sanità, Viale Regina Elena 299, 00161 Rome, Italy, ¶Centre for Molecular and Biomolecular Informatics, Nijmegen Centre for Molecular Life Sciences, Radboud University Nijmegen Medical Centre P. O. Box 9101, 6500 HB Nijmegen, The Netherlands, ||Department of Medical Microbiology/Parasitology, Radboud University Nijmegen Medical Centre, P. O. Box 9101, 6500 HB Nijmegen, The Netherlands, and \*\*Dipartimento di Biologia cellulare e Neuroscienze, Istituto Superiore di Sanità, Viale Regina Elena 299, 00161 Rome, Italy

Received, October 13, 2009, and in revised form, March 22, 2010  
Published, MCP Papers in Press, March 22, 2010, DOI 10.1074/mcp.M900479-MCP200

and PF14\_0748) (6). Interestingly, all such proteins and Pfs16 are localized in the gametocyte parasitophorous vacuole (PV)<sup>1</sup>, and some also are localized in the gametocyte-infected erythrocyte cytoplasm (6, 7). This suggests that, despite the overall similarities with an asexual trophozoite, the early gametocyte utilizes sexual stage-specific molecules to modify the PV and the host cell during gametocytogenesis. Compared with early gametocytes, purified mid- (III-IV) and mature (V) gametocytes stages were more deeply characterized in microarray and proteomics analyses, which altogether indicated that progression of sexual differentiation is accompanied by the up-regulation of 200–300 gametocyte-specific transcripts (8) and proteins (9, 10). Studies on the rodent malaria parasite *Plasmodium berghei* also indicated that a high proportion of the gametocyte proteins is specific for the proteome of the female or of the male gametocytes (11).

The aim of this work was therefore to obtain a genome-wide molecular characterization for the early gametocyte stages of *P. falciparum* by a quantitative comparative proteomics analysis of trophozoites and early and mature gametocytes. We developed a purification procedure for the isolation of early gametocytes that achieved purity better than 95% and allowed us to determine its proteome by liquid chromatography tandem mass spectrometry. Functional differences between early and late gametocytes were revealed by a gene set enrichment analysis (12) on semiquantitative expression data computed by an established peptide counting method (exponentially modified protein abundance index (emPAI)) (13). This work not only provided the first characterization of such virtually unknown stages of the parasite life cycle but also identified key cellular processes and molecules enriched in this early phase of gametocytogenesis.

#### EXPERIMENTAL PROCEDURES

**Parasites**—*P. falciparum* clones 3D7 (14) and F12 (15) were cultured in human O<sup>+</sup> erythrocytes provided from Prof. G. Girelli, Università La Sapienza, Rome, Italy, as described in Olivieri *et al.* (16). To obtain transgenic parasites, D-sorbitol-synchronized ring stage parasites were transfected as described in Olivieri *et al.* (16).

**Plasmids**—pHMC<sup>+</sup>/3R0.5 plasmid (17), kindly provided by Prof. A. Cowman, The Walter and Eliza Hall Institute of Medical Research, Melbourne, Australia, was modified to insert a genomic fragment of the *pf*g27 promoter and the TAA-less *pf*g27 coding sequence PCR-amplified with primers n.1 and .2 in supplemental Table S5. The *gfp* coding sequence and the *pf*g27 genomic downstream region were cloned from plasmid *p*27GFP (16), yielding plasmid pPfg27:GFP (supplemental Fig. S1). The plasmid for expressing a GST-fused

fragment of the PfgEXP10 protein in bacteria was obtained by cloning a 297-bp intronless genomic region of the *pf*gexp10 (PFA0670c) gene coding sequence in a BamHI/NotI-digested pGEX-6P-3 vector (Amersham Biosciences) with primers pfgEXP10 dir (GGATCCACTTCG-GTATCTTATAGTGATGAAGG) and pfgEXP10 rev (GCGGCCGCTC-TATATCTCTTTTCAGTGGATGCC relevant restriction sites are underlined in the primer sequences). Insertion in the final expression vector pGST-GEXP10 was controlled by sequencing. PCR amplification was carried out with Accuzyme DNA polymerase (Bioline) with conditions described in Olivieri *et al.* (16).

**Purification of Parasite Stages**—3D7/pPfg27:GFP Percoll-purified schizonts were used to start a culture in which gametocytogenesis was induced by a 5–8% increase in hematocrit. One day after stressed parasites appeared, a multilayer Percoll gradient (4) was used to eliminate schizonts and mature gametocytes. The resulting erythrocytes, ring stages, and early gametocytes were passed through a MACS (CS Miltenyi) column to retain the hemozoin-containing stage I-II gametocytes, which, eluted from the column, were fluorescence-activated cell sorter (FACS)-sorted to purify the fluorescent stage I-II gametocytes, detecting GFP emission by a 530-nm band pass filter, and gating on forward/side light scatter. Routinely  $7 \times 10^6$ – $1 \times 10^7$  parasites were purified; centrifuged in PBS, 2% BSA at 2000 rpm for 20 min; and frozen at –80 °C. For the trophozoite sample, synchronous trophozoites of gametocyte-less clone F12 (15) from a high parasitemia culture were MACS-purified.  $2.9 \times 10^7$  NF54 stage V gametocytes, cultured in a semiautomated culture system (18), were purified by Percoll gradient centrifugation (4).

**Sample Preparation for LC-MS/MS Experiments**—Cells were lysed by a freeze/thawing procedure as described in Lasonder *et al.* (9) and divided in a soluble, a wash, and a pellet fraction. Protein mixtures samples were solubilized in SDS-PAGE loading buffer and separated by SDS-PAGE on a 10% gel. Gels were stained with Coomassie G-250 (Bio-Rad) and cut into 10 slices per cellular fraction. Gel slices were treated with DTT and iodoacetamide and digested by trypsin as described in Lasonder *et al.* (9). Digested samples were acidified to a final concentration of 0.1% TFA and purified by stop and go extraction tips (19).

**Liquid Chromatography Tandem Mass Spectrometry**—Peptide identification experiments were performed using a nano-HPLC Agilent 1100 flow system connected on line to a 7 Tesla linear ion trap (LTQ) ion cyclotron resonance FT mass spectrometer (Thermo Fisher, Bremen, Germany). Digested samples were measured up to three times to increase the number of low abundance protein identifications. Peptides were separated on 15 cm 100  $\mu$ m-inner diameter PicoTip columns (New Objective, Woburn, MA) packed with 3  $\mu$ m Reprosil C<sub>18</sub> beads (Dr. Maisch GmbH, Ammerbuch, Germany) using a 90 min gradient from 12% buffer B to 40% buffer B (buffer B contained 80% acetonitrile in 0.5% acetic acid) with a flow rate of 300 nl/min. Peptides eluting from the column tip were electrosprayed directly into the mass spectrometer with a spray voltage of 2.0–2.2 kV. Data acquisition with the LTQ-FT instrument was performed in a data-dependent mode to automatically switch between MS and MS2. Full-scan MS spectra of intact peptides (*m/z* 350–1500) with an automated gain control accumulation target value of 1,000,000 ions were acquired in the Fourier transform ion cyclotron resonance cell with a resolution of 50,000. The four most abundant ions were sequentially isolated and fragmented in the linear ion trap by applying collisionally induced dissociation using an accumulation target value of 10,000, a capillary temperature of 100 °C, and a normalized collision energy of 27%. A dynamic exclusion of ions previously sequenced within 180 s was applied. All unassigned charge states and singly charged ions were excluded from sequencing. A minimum of 500 counts was required for MS2 selection.

**Peptide Identification by Mascot Database Searches**—Raw spectrum files were converted into Mascot generic peak lists by MaxQuant

<sup>1</sup> The abbreviations used are: PV, parasitophorous vacuole; MACS, magnetic activated cell sorter; emPAI, exponentially modified protein abundance index; GSEA, gene set enrichment analysis; PEXEL, *Plasmodium* export element; FACS, fluorescence-activated cell sorter; LTQ, linear ion trap; FDR, false discovery rate; SOTA, self-organizing tree algorithm; GO, gene ontology; ES, enrichment score; FWER, family-wise error rate; Bis-Tris, 2-[bis(2-hydroxyethyl)amino]-2-(hydroxymethyl)propane-1,3-diol; IFA, immunofluorescence analysis; PVM, PV membrane; BP, band passfilter.

(20) version 1.0.12.22. Proteins were identified by searching peak lists containing fragmentation spectra with Mascot version 2.2 (Matrix Science) against a the *P. falciparum* database (version 5.5, 5635 sequences) supplemented with the human International Protein Index database (version 3.52, 73,928 sequences) and frequently observed contaminants and concatenated with reversed copies of all entries. Mascot search parameters for protein identification specified an initial mass tolerance of 30 ppm for the parental peptide and 0.5 Da for fragmentation spectra and a trypsin specificity allowing up to three miscleaved sites. Carbamidomethylation of cysteines was specified as a fixed modification, and oxidation of methionine and deamidation of glutamine and asparagine were set as variable modifications. The required minimal peptide length was set at 6 amino acids. Internal mass calibration of measured ions and peptide validation by establishing false discovery rates (FDRs) was performed by MaxQuant as described in Cox and Mann (20). A final absolute recalibrated mass tolerance for the parental peptide was determined at 10 ppm. We accepted proteins with an FDR better than 1% and multiply charged peptides with an FDR better than 1% and not more than three variable modifications based on the number of accepted identifications of the reversed protein sequences. For proteins identified by one peptide, we applied a more stringent threshold and accepted unmodified peptides with a Mascot score threshold of 40 that were unambiguously assigned to one protein by a Mascot peptide delta score larger than 10. Assigned fragmentation spectra of single peptide hits were extracted using the MSQuant software package and are provided in supplemental Fig. S4. Assembling of peptide sequences on protein groups was performed by maximum parsimony where proteins were considered identified by detection of at least one unique peptide. In only a few cases (15 of 2400), *P. falciparum* peptide sets were assigned to protein groups with more than one protein. Validated *P. falciparum* peptides were mapped to protein sequences of PlasmoDB version 5.5 using the software package Protein Coverage Summarizer to retrieve positional information of the peptides.

**Identified Peptide Count Analysis to Determine Protein Abundance Index Values**—To determine protein abundance values in our samples, validated mass spectrometric data were quantified by a peptide count analysis that computed emPAI values for all proteins (13). emPAI values were calculated according to the following formula.

$$\text{emPAI} = 10^{\text{PAI}} - 1 \text{ with } \text{PAI} = n_{\text{observed peptides}}/n_{\text{observable peptides}} \quad (\text{Eq. 1})$$

The number of “observable” peptides per protein was calculated from the output of the program Protein Digestion Simulator, which computes peptide masses and hydrophobicities of simulated digests of protein databases. Protein emPAI abundance values were calculated from merged peptide lists for three samples (trophozoites, stage I-II gametocytes, and stage V gametocytes) and were normalized between different life cycle stages by the median emPAI abundance value as reported in Lasonder *et al.* (21).

**Self-organizing Tree Algorithm (SOTA) Clustering Analysis**—Relative emPAI expression profiles of proteins detected by at least two peptides in one of the life cycle stages (2211 of 2400 identified proteins) were clustered using The Institute of Genomic Research MultiExperiment Viewer (MeV4.2) software package (22). A SOTA by Euclidean distance was used with the following settings: for growth termination criteria: maximum cycles, 10; maximum epochs/cycle, 1000; maximum cell diversity, 0.01; minimum epoch error improvement, 0.0001; for centroid migration and neighborhood parameters: winning cell migration weight, 0.01; parent cell migration weight, 0.005; sister cell migration weight, 0.001, neighborhood level, 5; and for cell division criteria: cell variability,  $p = 0.05$ .

**Gene Set Enrichment Analysis (GSEA)**—GSEA statistically tests whether expression of a predefined group of genes (gene sets) correlates between cellular states and does not define subsets based on

expression levels prior to the statistical test (12); therefore, it is more sensitive than gene ontology (GO) enrichment tests. In total, 433 gene sets were collected from different sources with a minimal number of 15 genes per set. Gene sets were constructed from *P. falciparum* GO annotations. Gene ontology v1.2.obo and gene\_association.GeneDB\_Pfalciparum\_20080928 were downloaded from the GO consortium web site for mapping genes to GO terms and their parental GO terms using Ontologizer. GO terms based on ontology-based pattern identification clusters obtained from *Plasmodium* expression data and literature mining (23) were included in the gene sets as well. In addition, manually curated *Plasmodium* pathways were retrieved from PlasmoDB and added to the gene sets. Finally, the predicted conserved *Plasmodium* exportome from Sargeant *et al.* (24), the enriched gametocyte stage I-II proteins, and the enriched gametocyte stage V proteins identified in the above SOTA analysis were added. Expression data were  $\log_2$ -transformed to obtain a normal distribution required for the Pearson metric ranking method built into the GSEA v2.0 package.

The goal of the GSEA method is to determine whether members of a predefined gene set are randomly distributed around the ranked expression list or whether they are largely located around the top or bottom of that list. The enrichment score (ES) of a gene set is calculated by increasing a running sum statistic when one of the gene set members is found on the ranked list and by decreasing the running sum statistic when it is not encountered. We used a Pearson metric for ranking genes combined with a weighted method in the running sum statistics. For each gene set, the statistical significance (nominal  $p$  value) of the ES is estimated by a gene set-based permutation test procedure repeated 1000 times to generate a null distribution for the ES. The nominal  $p$  value is then calculated relative to this null distribution. To account for multiple testing of 433 gene sets, the significance level is adjusted by calculation of an FDR or a family-wise error rate (FWER) of normalized enrichment scores. We applied the most conservative multiple testing correction by a significance threshold or  $\text{FWER} < 0.05$  because of the low number of expression data sets: one data set of gametocyte stage I-II and one data set of gametocyte stage V. For the gene sets that passed the significance threshold, leading edge subsets, which define members participating particularly in biological processes, were calculated in the GSEA software package by the integrated leading edge analysis tool. Leading edge subsets are defined as those genes in the tested gene set that appear at the top or bottom in the ranked list before the point where the running sum reaches its absolute maximum. The leading edge subset is seen as the core of a gene set that accounts for the enrichment signal in GSEA and is used to assess overlap between gene sets in the enrichment analysis.

**Determination of N-terminal Acetylated Plasmodium Export Element (PEXEL) Motif-containing Peptides**—Putative exported proteins that contain PEXEL (RX(L/I)X(D/E/Q)) motifs (25) were downloaded from PlasmoDB (1444 proteins). A refined protein set of putatively exported PEXEL motif-containing proteins based on *Plasmodium* species conservation (475 proteins) was obtained from Sargeant *et al.* (24), and a second refined data set based on proteins with a predicted PEXEL motif plus a preceding hydrophobic region (411 proteins) was taken from Hiss *et al.* (26).

Mascot search parameters for acetylated peptide identification specified an initial mass tolerance of 30 ppm for the parental peptide and 0.5 Da for fragmentation spectra and a semitrypsin specificity allowing up to two miscleaved sites. Carbamidomethylation of cysteines was specified as a fixed modification, and acetylation of lysine and the peptide N terminus, oxidation of methionine, and deamidation of glutamine and asparagine were set as variable modifications. Only peptides that contain a C-terminal tryptic site were considered for subsequent verification analysis by the MaxQuant software package.

The assignment in MS2 spectra of individual modifications sites was scored automatically using the posttranslational modification algorithm (27) also implemented in MaxQuant and finally verified by manual inspection of MS2 spectra (spectra are provided in supplemental Fig. S5). N-terminally acetylated peptide sequences were mapped on protein sequences that contain PEXEL motifs, and the set of N-terminal acetylated peptides within the PEXEL domains represent PEXEL proteins that show an *N*-acetyltransferase substrate sequence as reported for PfEMP2 (28).

**Production of GST Fusion Proteins and Mouse Immunization**—Expression of GST from plasmid pGEX-6P-3 and of the GST-GEXP10 fusion protein from pGST-GEXP10 was induced in *Escherichia coli* BL21 by 1 mM isopropyl  $\beta$ -D-galactopyranoside for 2 h at 37 °C. BugBuster Protein Extraction Reagent (Novagen) was used for protein extraction. Purification of the GST fusion protein from soluble fraction was achieved using glutathione-Sepharose 4 Fast Flow resin (Amersham Biosciences) according to manufacturer's instructions. SDS-PAGE analysis showed that the GST fusion protein could be eluted as a highly purified protein. Immunizations were carried out with BALB/c mice under the guidelines of Istituto Superiore di Sanità, conforming to European Commission directive 86/609 regulating ethical issues on laboratory animal treatment. Two mice were subsequently immunized intraperitoneally with 40, 20, 20, and 10  $\mu$ g of purified fusion protein in a total volume of 300  $\mu$ l formulated in Freund's adjuvant on days 0, 28, 42, and 56, respectively. On day 0, prebleed samples were taken as preimmune sera. The final bleed was 7 days after the last immunization.

**Western Blot Analysis**—Protein extracts from Percoll-purified gametocytes ( $10^7$ /lane) were obtained by lysis in 10 mM Tris-Cl, pH7.5, 50 mM NaCl, 5 mM EDTA, 1% Triton X-100, 0.05% SDS, 0.1 mM PMSF supplemented with Complete protease inhibitor mixture (Roche Applied Science). Soluble and insoluble fractions were separated by gradient gel electrophoresis on Bis-Tris 4–12% gels (Novex). Transfer of separated proteins onto a nitrocellulose filter (Protran, 0.2  $\mu$ m) was performed by electroblotting for 1 h at 350 mA. Membranes were incubated for 1 h with the anti-PfGEXP10 antibody at a 1:500 dilution. Horseradish peroxidase-conjugated secondary antibody against mouse IgGs was diluted 1:30,000, and the chemiluminescent reaction was revealed with the Super Signal West Substrate kit (Pierce).

**Immunofluorescence Analysis**—Parasites were fixed in suspension with 4% paraformaldehyde, 0.075% glutaraldehyde and permeabilized with 0.1% Triton X-100 as described in Tonkin *et al.* (29). After a 30-min preincubation in 1% BSA, parasites were incubated with the anti-PfGEXP10 or the anti-GST mouse antibody (1:100) and the anti-Pfmdv-1/peg3 rabbit antiserum (7). After incubation and washes in  $1 \times$  PBS, parasites were incubated with an affinity-purified, rhodamine-conjugated secondary antibody against mouse or rabbit IgGs diluted 1:200 and Hoechst at 1  $\mu$ g/ml for nuclear staining. After the final washes, samples were observed at  $100\times$  magnification in a Leitz DMR fluorescence microscope equipped with the following filters: BP 340–380 (Hoechst), BP 515–560 (rhodamine), and BP 470–490 (fluorescein). Images were collected with a Leica cooled charge-coupled device camera and deconvolved using the AutoDeblur software (AutoQuant Imaging, Inc.).

## RESULTS

**Preparation of Purified, Stage-specific *P. falciparum* Samples**—As reliable blood stage proteome determination critically depends on sample purity, targeted strategies were separately applied to obtain highly pure synchronized parasites for the three blood stages. To obtain gametocyte-free trophozoites of *P. falciparum*, we used parasite clone F12, a 3D7A

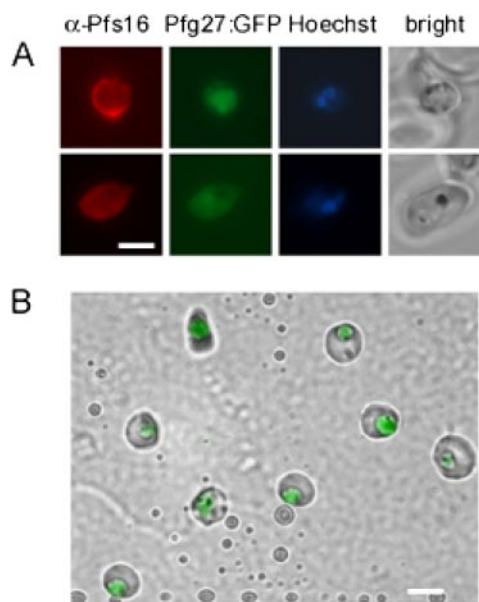


**FIG. 1. Fluorescent *P. falciparum* early gametocytes for proteomics analysis.** A, stage I (top) and II (bottom) gametocytes expressing the Pfg27-GFP fusion protein (green) stained with a monoclonal antibody specific for the early gametocyte protein Pfs16 (red fluorescence). Nuclei were stained with Hoechst. Bar, 5  $\mu$ m. B, sample of FACS-sorted parasites showing highly purified stage I and II gametocytes. Bar, 10  $\mu$ m.

derivative unable to produce the earliest detectable gametocyte stages (15). Synchronous trophozoites from F12 high parasitemia cultures were MACS-purified, and  $8 \times 10^7$  parasites were analyzed by mass spectrometry. To obtain mature stage V gametocytes, routine Percoll purification of mature gametocyte cultures previously treated with *N*-acetylglucosamine to clear residual asexual parasites (30) produced a sample of  $2.9 \times 10^7$  parasites free of asexual stages.

To obtain purified early gametocytes, a *P. falciparum* 3D7A line was obtained that expresses GFP specifically in gametocytes and from an early stage of sexual differentiation. The GFP coding sequence was fused with that of the early gametocyte protein Pfg27 (4) under the control of *pfg27* genomic flanking sequences in plasmid pPfg27:GFP (supplemental Fig. S1). Parasite line 3D7/pPfg27:GFP was obtained after transfection and selection of WR99210-resistant parasites. The *pfg27* flanking sequences in the plasmid produced, as expected (16), GFP fluorescence only in morphologically recognizable gametocytes and in round shaped stage I gametocytes from  $\sim 40$  h post invasion. Immunofluorescence analysis (IFA) confirmed the identity of the latter cells as all GFP fluorescent round shaped parasites were also positive for the early gametocyte marker Pfs16 (Fig. 1A). To achieve the purity required for proteome analysis, a three-step protocol was developed to purify fluorescent early gametocytes from the 3D7/pPfg27:GFP line. As diagrammatically shown in supplemental Fig. S2, a Percoll gradient was used to eliminate mid-/late stage gametocytes and schizonts. Passage of the

remaining cells through a MACS column retained pigmented early gametocytes and small trophozoites from ring stages and uninfected red blood cells. Finally, FACS purified the GFP-positive young sexual stages from the non-fluorescent trophozoites. This protocol routinely yielded  $\geq 95\%$  pure preparations of stage I/early stage II gametocytes with less than 5% contamination of asexual parasites (ring or trophozoite stages) or uninfected red blood cells as determined by cytofluorimetric (supplemental Fig. S2) and microscopic (Fig. 1B) examination. Two samples of  $7 \times 10^6$  and  $1.8 \times 10^7$  cells were prepared with this protocol and subjected to mass spectrometry analysis.

**Liquid Chromatography-Tandem Mass Spectrometry Determination of Three Parasite Blood Stage Proteomes**—Protein samples from the above parasite preparations were analyzed by high mass accuracy nano-LC-MS/MS, previously applied to analysis of infected blood (9) and mosquito stages (21), with a more sensitive and accurate mass spectrometer. To accomplish in-depth proteomes, proteins were size-fractionated by one-dimensional SDS-PAGE into 10 gel slices per cellular fraction (either pellet or cytosolic), and tryptic digests of these slices were measured by LC-MS/MS in triplicate. We used an LTQ-FT ICR mass hybrid mass spectrometer to acquire parent ion masses with mass accuracies smaller than 30 ppm in the ICR cell and to acquire fragment ions within 400 ms in the ion trap. Iterative calibration algorithms were used by the MaxQuant software package to achieve an average absolute mass accuracy of 2.00 (s.d. 1.74) ppm for all identified peptide ions. The acquired MS/MS spectra were searched against a combined database of all possible predicted tryptic peptides derived from all *P. falciparum* and human proteins. Stringent validation criteria for protein identifications established a protein false discovery rate less than 1% by reverse database searches.

The proteomics analysis of *P. falciparum* trophozoites, early stage I-II gametocytes, and mature stage V gametocytes resulted in a total of 26,351 unique peptides mapping to 2400 non-redundant *P. falciparum* proteins across the three life cycle stages: 1345 in trophozoites, 1427 in early gametocytes, and 2031 in mature gametocytes (Fig. 2A and supplemental Table S1). The early stage gametocyte proteome was determined from two batches of FACS-purified parasites of  $7 \times 10^6$  and  $1.8 \times 10^7$  cells. These batches identified 653 and 1418 proteins, respectively; 644 proteins were shared. Only nine proteins (1.4% of the total) of the gametocyte batch of  $7 \times 10^6$  cells were not found in the larger batch of  $1.8 \times 10^7$  cells, demonstrating a low degree of random sampling variation between samples. Such a random variation may thus account for at least some of the 95 proteins detected only in early gametocytes (Fig. 2A) that therefore may not be confidently considered as specific for such a stage solely on the basis of the proteomics analysis. Finally, this analysis identified a total of 1090 proteins not detected in previously published determinations of the proteomes of tro-

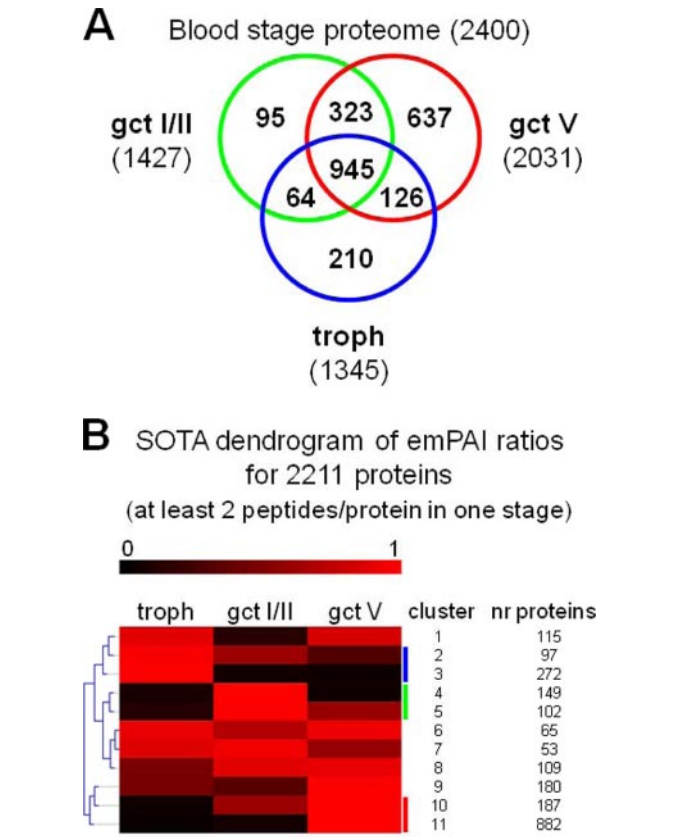


FIG. 2. Proteomes of early and mature gametocytes and of asexual trophozoites. **A**, Venn diagram of the proteins identified in the proteomes of the three parasite stages. **B**, dendrogram from the SOTA clustering analysis on the relative emPAI profiles of 2211 proteins distributed across the three developmental stages. Vertical colored bars mark clusters of the proteins enriched in the three parasite stages (blue, trophozoites (*troph*); green, early gametocytes (*gct I/II*); red, mature gametocytes (*gct V*)). *nr*, number.

phozoites and gametocytes restricted to the identification of fully tryptic peptides (9, 10).

**Cluster Analysis of Protein Abundance Profiles**—The majority of proteins (1459 of 2400) were detected in more than one life cycle stage (Fig. 2A). To reveal quantitative differences of protein levels between stages, we computed protein abundance values using the emPAI peptide counting method (13), previously successfully applied to analyze *P. falciparum* mosquito stage proteome data (21). To identify groups of proteins with similar relative expression profiles, we computed emPAI values for proteins detected by at least two peptides in at least one of the three parasite stages (2211 of 2400). Profiles of emPAI relative abundances for such proteins were analyzed by SOTA clustering (22), which identified 11 clusters. These were manually assembled in four categories containing proteins enriched in trophozoites (369 proteins from SOTA clusters 2 and 3), enriched in early gametocytes (251 proteins in clusters 4 and 5), enriched in mature gametocytes (1069 proteins in clusters 10 and 11), and shared between the three

TABLE I  
GSEA of early gametocyte-enriched proteome

NES, normalized enrichment score; LES, leading edge subset; gct I/II, gametocyte I/II.

Name and description of gene set <sup>a</sup>	Size <sup>b</sup>	NES	p value	FDR q value	FWER p value	LES
						%
gct I-II-enriched	251	-15.4829	<0.001	<0.001	<0.001	100
Exportome <i>Plasmodium</i> -conserved	65	-5.17703	<0.001	<0.001	<0.001	75
Genes coding for chaperones and their regulators	74	-3.24795	<0.001	<0.001	<0.001	62
OPI_GO:PM15591202_Trp: targeting malaria virulence and remodeling proteins to the host erythrocyte	147	-3.10504	<0.001	<0.001	<0.001	65
Genes coding for components involved in ribosome assembly	33	-2.75754	<0.001	3.6 × 10 <sup>-4</sup>	0.004	79
OPI_GO:0004386: helicase activity	90	-2.56926	<0.001	0.001	0.025	61

<sup>a</sup> See “Experimental Procedures” for gene set construction.

<sup>b</sup> Number of genes.

stages (522 proteins in clusters 1 and 6–9) (Fig. 2B and supplemental Table S2). In conclusion, this quantitative comparative analysis identified constitutive and enriched or possibly specific proteins produced in asexual trophozoites, in mature gametocytes, and, for the first time, in early gametocytes.

**Validation of Young and Mature Gametocyte-enriched Proteomes**—The proteomes of the early and the mature gametocytes were inspected for the presence of previously characterized gametocyte proteins. Proteins Pfg377 (PFL2405c), PfsMR5 (PFB0400w), and Pfs25 (PF10\_0303), respectively produced from stage III gametocytes, stage V gametocytes, and gametes (31–33) were not detected in the early gametocyte proteome but only in that of mature stages. Conversely, proteins Pfg27 (4), Pfg14.744, Pfg14.748 (6), and Pfmdv-1/peg3 (5, 7), abundantly produced in stage I-II gametocytes, were predominantly represented in the early gametocyte proteome. Besides validating the stage specificity of the gametocyte samples, this analysis also provided information on the expression of other reference proteins. Protein Pfs16, expressed from early gametocytogenesis (3), the sexual stage-specific tubulin  $\alpha$ -II (PFD1050w), and the fertilization proteins Pfs230 (PFB0405w) and Pfs45/48 (PF13\_0247), reported to appear from stage II to stage III gametocytes (34, 35), were all overrepresented in the proteome of mature gametocytes, indicating that their early appearance in sexual differentiation is followed by a significant accumulation in later stages of gametocyte maturation. Analysis of eight gene products encoded by a subtelomeric region of chromosome 9 reported to be involved in cytoadherence, gametocytogenesis (36), and host cell remodeling (37) revealed that five, PFI1715w, PFRex-3 (PFI1755c), PFRex-4 (PFI1760w), PFI1770w, and PFI1800w, were enriched in early gametocytes, whereas PFRex-1 (PFI1735c), PFCLAG9 (PFI1730w), and PFI1780w were instead overrepresented in asexual trophozoites, possibly suggesting that such proteins play specific roles in such processes in the two developmental stages. Finally, of 106 gene products up-regulated in the transcriptome of late gametocytes annotated with GO function “*Plasmodium* sexual

development” (8), 88.6% were overrepresented in (and 64% were specific for) mature gametocytes, confirming that functions of these genes are likely to be relevant for the late phases of gametocyte maturation.

**Functional Characterization of Early Gametocyte Proteome by Gene Set Enrichment Analysis**—To reveal pathways or processes associated specifically to the early phase of gametocytogenesis, a functional annotation of the 251 proteins overrepresented in this proteome was performed by GSEA, which is widely used for the analysis of microarray data. We applied this method as it is very sensitive to detect subtle differences between cellular states that may escape detection by other gene ontology enrichment analyses (12). The GSEA analysis identified six overrepresented gene sets in early gametocytes (Table I and supplemental Table S4) using a conservative significance threshold of FWER < 0.05. The most significantly represented set, besides the expected stage I-II gametocyte gene set control, was that of genes encoding predicted *Plasmodium* exported proteins (24), the second was that of chaperone proteins, and the third was that of gene products putatively involved in host cell remodeling (25). Therefore, the three most enriched gene sets were related to protein export, host cell remodeling, and chaperonins. A role for chaperonins in such processes was recently reported in Botha *et al.* (38). To independently confirm this finding, the presence of proteins containing the PEXEL domain or host targeting signal (24) was statistically analyzed in the early and mature gametocyte proteomes. A Fisher exact test showed a 2.2-fold enrichment of exported proteins in the enriched/specific proteome of stage I-II gametocytes compared with the total proteome of such stages (19 PEXEL-containing proteins in the 251 proteins of the early gametocyte-enriched/specific proteome versus a total of 50 PEXEL-containing proteins in the 1432 proteins detected in these stages;  $p = 0.009$ ). In contrast, the same analysis showed a 3.2-fold depletion of such proteins in the stage V gametocyte-enriched/specific proteome (7 of 1069 in the enriched/specific proteome versus 42 of 2033 in the total proteome;  $p = 0.002$ ). Thus, the above analyses altogether demonstrated that proteins predicted to

be exported in the erythrocyte cytoplasm and putatively involved in host cell remodeling are predominantly represented in early sexual stages, providing evidence that this process marks the early phase of gametocytogenesis in *P. falciparum*.

**Proteins Putatively Involved in Host Cell Remodeling in Early Gametocyte Maturation**—The above analysis altogether identified 63 putatively exported proteins in the full early gametocyte proteome (Table II). Of these, 37 were either shared with at least another stage or detected by one peptide only. SOTA analysis (described above) on the normalized emPAI values across the three stages indicated that 26 of these proteins were instead overrepresented or detected only in the early gametocyte proteome. This result suggested that these 26 proteins represent a subset of putatively exported protein candidates that play specific roles in host cell remodeling in early gametocytes, and they were therefore named *P. falciparum* gametocyte exported proteins (PfGEXPs). Importantly, these include proteins previously demonstrated to be exported in early gametocytes, Pfg14.744 and Pfg14.748 (6), or in early asexual parasites, PfRex-3 (37). Comparative analysis provided further clues on differences in protein export between asexual and sexual stages. As described for early gametocytes, also the proteome of asexual trophozoites, well known to actively remodel their host cell, contains 54 putatively exported proteins enriched or specific for such stages (in a total of 75 detected in this proteome), suggesting that protein export in asexual and early sexual development may present significant functional differences. In this respect, we noticed that five of the eight proteins required for the processing or the export of the polymorphic parasite adhesin PfEMP1 or the formation of adhesion-related knob structures in asexual parasites (39) were enriched in the trophozoite proteome with only MAL7P1.172 (PfGEXP11) overrepresented in the early gametocyte proteome. This suggests that such processes are predominantly related to asexual development despite previous work describing an asexual-like mechanism of cytoadherence and the presence of knobs in stage I gametocytes (40).

Finally, the presence of the molecular machinery recently proposed to process (41, 42) and translocate (43) PEXEL-containing proteins in asexual parasites was also investigated. This revealed that protease Plasmepsin V (PF13\_0133) was present in all stages and overrepresented in trophozoites and that four of five components of the putative translocon were present indeed in our proteome data: PTEX150 (PF14\_0344) was enriched in the early gametocyte sample, HSP101 (PF11\_0175) and EXP2 (PF14\_0678) were enriched in the trophozoite sample, whereas TRX2 (MAL13P1.225) was shared across all stages (supplemental Table S2).

**Mass Spectrometric Identification of PEXEL Processing and N-Acetylated Termini of Endogenous Parasite Proteins**—Most exported proteins in *Plasmodium* contain the conserved PEXEL motif (RXLX(E/Q/D)) that has been shown to contain a classical N-acetyltransferase substrate sequence by mass

spectrometry (28, 44). To detect in our data set endogenous acetylated protein N termini cleaved at the PEXEL motif, the LC-MS/MS data were inspected using Mascot with semitrypsin enzyme specificity. Importantly, we re-searched a global data set that enabled finding a small fraction of all processed protein N termini. This analysis identified 14 proteins (Table III, supplemental Table S3, and supplemental Fig. S5) in which, in all cases, N-acetylation takes place at position 4 of the PEXEL motif, providing a mass spectrometry-based evidence of this modification in endogenous protein and confirming the identification of N-acetylated PEXEL peptides recently reported for proteins PF11780w, PFE0050w, and PfEMP2 (PFE0040c) (28, 44). Interestingly, all modified proteins were detected in the early gametocyte and/or in the trophozoite proteomes, and none were detected in that of mature gametocytes. Three of the identified modified proteins were enriched in early gametocytes: Pf14.744, PfRex-3, and PfGEXP10, whose CID fragmentation spectrum is shown in Fig. 3A. As mentioned above, export has been reported for Pfg14.744 in gametocytes (6) and for PfRex-3 in ring stage parasites (37), and our detection of PEXEL cleavage and N-acetylation of these proteins provides a further insight into the molecular mechanism responsible for their trafficking in the host cytoplasm.

**A novel Parasite Protein Exported in Gametocyte Development**—To investigate the possible export of the third gametocyte-enriched protein, PfGEXP10 (PFA0670c), shown above to be cleaved and N-acetylated at its PEXEL motif, we raised antibodies on a portion of the protein fused to GST (supplemental Fig. S3) and used them to characterize its production and localization in gametocyte development. The anti-PfGEXP10 serum and a control serum against GST were used in Western blot and IFAs on 3D7 gametocytes. In Western blot, anti-GST antibody failed to detect any parasite specific band, whereas the anti-PfGEXP10 serum recognized a band at 17–20 kDa, predominantly in the parasite soluble fraction, at a molecular mass compatible with that of the protein processed at its PEXEL sequence (Fig. 3, B and C). The anti-PfGEXP10 antibody was also used in IFA on paraformaldehyde/glutaraldehyde-fixed, permeabilized gametocytes at different stages of maturation. To visualize the possible export of PfGEXP10, the gametocyte PV membrane (PVM) was simultaneously labeled with an antiserum specific for the gametocyte PVM protein Pfmdv-1/peg3 (5, 7). Unlike the anti-GST control antiserum, the anti-PfGEXP10 antiserum reacted with stage I and mid-stage gametocytes and clearly showed a punctate fluorescence pattern beyond the PV compartment (Fig. 3D). Specific staining in the erythrocyte cytoplasm was barely observable in stage I gametocytes, and it was far more evident in later maturation stages, indicating that the PfGEXP10 protein is indeed exported in the erythrocyte cytoplasm during gametocyte development.

TABLE II  
*Putatively exported proteins in early gametocyte proteome*

PlasmoDB ID	Exportome annotation	PEXEL start residue	PEXEL end residue	Motif (according to Ref. 24)	Stage enrichment	PfGEXP name (or previous annotation)
PFL2550w	dnaj_III	35	59	RILSD	Early gametocytes	PfGEXP01
PF11_0037	PHISTb <sup>a</sup>	65	89	RNLYE	Early gametocytes	PfGEXP02
PF14_0275	Unique	52	76	RLLCT	Early gametocytes	PfGEXP03
MAL13P1.475	PHISTb	81	105	RSLLG	Early gametocytes	PfGEXP04
PF11770w	PHISTb	73	97	RKLSE	Early gametocytes	PfGEXP05
PFA0675w	dnaj_III	213	217	RILYS	Early gametocytes	PfGEXP06
MAL13P1.61	hyp8	36	60	RSLAE	Early gametocytes	PfGEXP07
MAL7P1.178	ab_hydb				Early gametocytes	PfGEXP08
MAL8P1.2	PHISTb				Early gametocytes	PfGEXP09
PFA0670c	hyp8	42	66	RWLSE	Early gametocytes	PfGEXP10
MAL7P1.172	PHISTc	79	103	RNLGE	Early gametocytes	PfGEXP11
PF11_0503	PHISTc	35	59	RTLAS	Early gametocytes	PfGEXP12
MAL8P1.205		58	82	RKLSE	Early gametocytes	PfGEXP13
PF11_0038	Unique	81	105	RLLCE	Early gametocytes	PfGEXP14
PF10_0310	hyp2				Early gametocytes	PfGEXP15
PF14_0075	Unique	55	79	RKLYQ	Early gametocytes	PfGEXP16
PF14_0752	PHISTa	55	79	RNLTE	Early gametocytes	PfGEXP17
PFD0115c	Unique	49	73	RILVE	Early gametocytes	PfGEXP18
PFA0550w	Unique	106	130	KRICK	Early gametocytes	PfGEXP19
PFB0900c	PHISTc	74	78		Early gametocytes	PfGEXP20
PFC0080c	hyp1	131	135	RLLAQ	Early gametocytes	PfGEXP21
PF11715w	Unique	86	90	RNLAE	Early gametocytes	PfGEXP22
PF14_0744	Unique	53	57	RSLSE	Early gametocytes	Pfg14-744
PF14_0748	PHISTa	116	120	RNLTE	Early gametocytes	Pfg14-748
PF11755c	Unique	36	60	RQLSE	Early gametocytes	Pfref-3
PF11760w	Unique	35	59	RNLSE	Early gametocytes	Pfref-4
MAL7P1.171	emp3	77	101	RSLTE	Trophozoites	
MAL8P1.4	PHISTc	64	88	RILYE	Trophozoites	
PF07_0087	Unique	51	75	RKLLS	Trophozoites	
PF08_0137	PHISTc				Trophozoites	
PF10_0023	hyp16	77	101	RFLSE	Trophozoites	
PF10_0025	hyp16	47	71	RLLSE	Trophozoites	
PF10_0159	gbp130	74	98	RILAE	Trophozoites	
PF11_0052	Unique	48	72	RNITE	Shared	
PF11_0099	Unique	46	70	RQLAK	Shared	
PF11_0508	Unique	76	100	RVLYD	Trophozoites	
PF11_0509	PHISTb_dnaj	75	99	RNLYC	Trophozoites	
PF13_0076	Unique	81	105	RSLSE	Trophozoites	
PF13_0218					Mature gametocytes	
PF13_0275	Unique	76	100	RILTQ	Trophozoites	
PF13_0317					Mature gametocytes	
PF14_0553	Unique	73	97	RVLLE	Mature gametocytes	
PFA0110w	PHISTb_dnaj	273	277		Trophozoites	
PFA0210c	Unique	60	64		Trophozoites	
PFA0225w	Unique	55	79	RSILQ	Mature gametocytes	
PFA0300c	Unique	119	123	RLLGS	Shared	
PFB0085c	PHISTb_dnaj	42	66	RQLSE	Trophozoites	
PFB0090c	dnaj_I	44	48		Trophozoites	
PFB0106c	Unique	92	116	RSLAE	Trophozoites	
PFB0915w	Unique	88	92		Trophozoites	
PFB0920w	PHISTb_dnaj	122	126	RSLCE	Not determined <sup>b</sup>	
PFC0085c	Unique	76	100	KSLAE	Trophozoites	
PFD0095c	PHISTb	41	65	RKLYH	Trophozoites	
PFD1035w	unique	39	63	KNLKS	Shared	
PFD1170c	PHISTb	76	100	RILSE	Trophozoites	
PFE0050w	Unique	79	103	RVLAE	Trophozoites	
PFE0055c	dnaj_I	50	74	RSLAE	Trophozoites	
PFE0060w	unique	33	57	RTLAD	Trophozoites	
PFE1170w	dnaj_III				Shared	

Downloaded from <http://www.mcponline.org/> by guest on February 18, 2019

TABLE II—continued

PlasmoDB ID	Exportome annotation	PEXEL start residue	PEXEL end residue	Motif (according to Ref. 24)	Stage enrichment	PfGEXP name (or previous annotation)
PF11780w	PHISTc	47	71	KSLAE	Trophozoites	
PFL0040c	FIKK K			KCLSE	Not determined	
PFL0600w	Unique	26	50	RILKE	Shared	
PFL2565w	PHISTa	36	60	RNLAQ	Not determined	

<sup>a</sup> PHIST; Plasmodium helical interspersed subtelomeric family.

<sup>b</sup> Not determined, these proteins showed less than two peptides in each of the stages and were not included in the emPAI-based comparative analysis.

TABLE III

Detected *N*-acetylated protein termini within PEXEL motif

troph, trophozoites; gct I-II, early stage I-II gametocytes.

PlasmoDB ID	Annotation	Peptide mapping on PEXEL motif <sup>a</sup>	PEXEL position	Sample	Ref.
PF14_0744	Pfg14.744	<b>RSLSE</b> lvlanypssnyafsnayasanyssnyppsskm	53–57	gct I-II	
PF11755c	PfRex-3	<b>RQLSE</b> pvveeqdlkkt	45–49	gct I-II	
PFA0670c	PfGEXP10	<b>RWLSE</b> tsvsydegeplky	51–55	gct I-II	
PF11780w	PHIST <sup>b</sup> domain protein	<b>KSLAE</b> aspeehnnlrs	57–61	troph and gct I-II	31
PFE0050w	One transmembrane PEXEL protein	<b>RVLAE</b> qedqyirn	88–92	troph and gct I-II	31
PF11_0503	Hypothetical protein	<b>RTLAS</b> amqhsrlrg	45–49	troph and gct I-II	
PF10_0023	Protein with predicted PEXEL motif	<b>RFLSE</b> pllefdtvfdtflkn	86–90	troph and gct I-II	
PFE0060w	PIESP2 erythrocyte surface protein	<b>RTLAD</b> ndmfangkn	42–46	troph	
PFA0210c	Hypothetical protein, conserved	<b>RILKE</b> nkeesletaavnentkd	60–64	troph	
PF10_0023	Protein with predicted PEXEL motif	<b>RFLSE</b> pllefdtvfdvfkfkd <b>RFLSE</b> pllefdtvfdvfkdtflkn	86–90	troph	
PF14_0013	DnaJ protein, putative	<b>RNLSE</b> sgenhnsftrt	83–87	troph	
PFE0040c	PfEMP2	<b>RILSE</b> teppmsleeimrt	74–78	troph	32
MAL7P1.174	PHIST domain protein	<b>RILSE</b> veslqssnysevkmkn	51–55	troph	
MAL8P1.206	<i>P. falciparum</i> hypothetical protein, conserved	<b>RLLTE</b> imencslngrl	46–50	troph	

<sup>a</sup> See “Experimental Procedures” for PEXEL prediction sources. In bold, PEXEL motif; underlined, identified *N*-acetylated peptide.

<sup>b</sup> PHIST; Plasmodium helical interspersed subtelomeric family.

## DISCUSSION

This work provides the first comprehensive proteomics characterization of a largely unexplored part of the life cycle of *P. falciparum*, the early gametocyte stages at about 40–48 h of maturation after red blood cell invasion. This result could be achieved because we specifically developed a protocol able to obtain highly pure (>95%) preparative samples of stage I/early stage II gametocytes based on cell sorting of GFP-tagged parasites. Previous protocols obtained purification efficiencies of such trophozoite-like cells around 80% (8) by tight parasite synchronization, controlled overgrowth, and clearance of asexual parasites with *N*-acetylglucosamine, which were not necessary in the present protocol. In the past, genome-wide analyses of *P. falciparum* early gametocytes were achieved comparing gene expression in parallel cultures of parasite able and unable to enter gametocytogenesis (5, 6). Intrinsic biological variability and the unavoidable residual presence of unhealthy trophozoites were largely responsible for the poor overlaps between the gene lists obtained in those experiments. The possibility to obtain highly purified early gametocyte samples of *P. falciparum* and the present proteomics characterization now open the way to further cellular,

molecular, and biochemical analyses of this part of the parasite life cycle.

*Comparative Proteome Analysis Provides Clues to Functional Processes in Early Gametocytogenesis*—The improved performance of our mass spectrometry analysis with a severalfold increase in sensitivity, dynamic range, and sequencing speed compared with previous studies on sexual and asexual parasites (9, 10) allowed us to identify a total of 2400 non-redundant proteins in the three developmental stages, 1090 of which were undetected in previous parasite proteomics analyses, and to perform an in-depth quantitative comparative analysis of the proteome of the early gametocytes with those, newly determined here, of asexual trophozoites and mature gametocytes. Calculation of the relative protein abundance levels (emPAI values) for the proteins identified in the three stages and cluster analysis of the resulting profiles identified sets of proteins enriched in or possibly specific for the three developmental stages. The GSEA of the 251 gene products enriched in the early gametocyte proteome, against 400 gene sets from several general and *Plasmodium*-specific annotation sources, identified only five gene sets significantly over-represented in this proteome. Remarkably, the three sets with

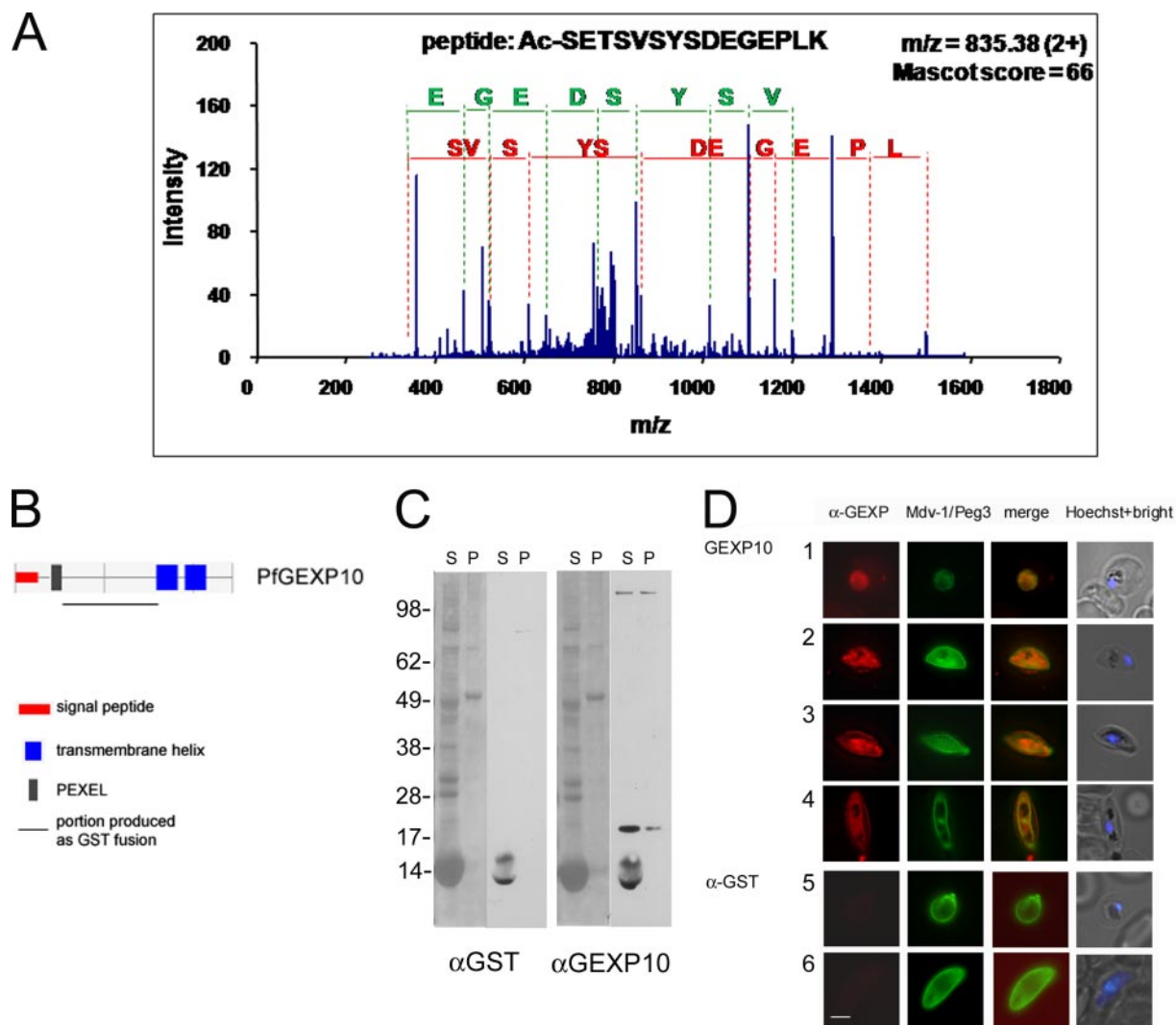


**FIG. 3. PfGEXP10 processing and export in gametocytogenesis.** *A*, mass spectrometry identification of the *N*-acetylated PfGEXP10 polypeptide after cleavage at its PEXEL motif. The *y*-ion fragment series are color-coded in *green*, and the *b*-ions are in *red*. *B*, primary structure of the PfGEXP10 protein according to PlasmoDB and Eukaryotic Linear Motif (ELM) database annotations. The PfGEXP10 portion produced as the GST fusion for generating specific antibodies is shown. *C*, Western blot analysis with anti-PfGEXP10 antibody on gametocyte extracts. Soluble (*S*) and insoluble (*P*) fractions from gametocyte extracts were electrophoresed, blotted, and detected with Ponceau S staining (*left side* of each panel). Blots incubated with the control anti-GST and the anti-PfGEXP10 antibodies are shown on the *right side* of each panel. *D*, IFA with anti-PfGEXP10 antibody on early and mid-stage gametocytes. Fixed, permeabilized 3D7 gametocytes were simultaneously incubated with the serum against the PfGEXP10 protein or a control anti-GST antiserum (*red* fluorescence) and a serum against the gametocyte PVM marker PfMdv-1/peg3 (*green* fluorescence). Nucleus-specific Hoechst staining is shown on the *right*. *1* and *5*, stage I; *2*, stage II; *3* and *6*, stage III; *4*, late stage IV. *Bar*, 5  $\mu$ m.

the highest significance values were those of genes encoding (i) conserved *Plasmodium* exportome proteins (24), (ii) chaperonins and their regulators, and (iii) proteins involved in host cell remodeling (25), all referring to functionally linked processes of protein export and host cell remodeling. Indeed, more than 10% of the proteins enriched in the early gametocyte proteome are represented by the 26 putatively exported proteins here identified and named PfGEXPs. Published evidence and results obtained in this study indicate that three of them, Pfg14.744, PfRex-3, and PfGEXP10, are indeed cleaved at the conserved leucine residue within their PEXEL

motif, *N*-terminally acetylated, and exported to the infected erythrocyte cytoplasm. Although further analysis is needed on other members of this gene group, these data strongly suggest that several such proteins are trafficked during gametocyte development.

*Active and Specific Protein Export in Early Gametocytogenesis*—This work reveals that the parasite protein export machinery is comparatively more active in the early phase of sexual differentiation than in mature gametocytes as PEXEL-containing proteins are overrepresented in the proteome enriched in early gametocytes and are, on the con-

trary, depleted in that of late gametocytes. Also, PEXEL processing and *N*-acetylation were detected only in the proteome data obtained from the early but not from the late gametocytes.

Our finding that protein export is highly active in early gametocytogenesis and recruits a significant set of gametocyte-enriched proteins opens questions on the physiological role of this process in sexual differentiation and on its differences with the analogous processes in asexual parasites required for parasite cytoadherence to the vascular endothelium and sequestration in various organs during infection (39). In this respect, two aspects of the gametocyte biology can be discussed where differences with asexual stage development are becoming increasingly evident: the role of the PV in gametocytogenesis and the sequestration properties of gametocytes. On the first issue, our results support at a genome-wide level previous hypotheses of major, stage-specific modifications of the parasite PV in early gametocytogenesis based on the observation that five of the six early gametocyte proteins identified prior to the present analysis, Pfs16 (3), Pfmdv-1/peg3 (5, 7), Pfpeg4 (5), Pfg14.744, and Pfg14.748 (6), are exported to or beyond the parasitophorous vacuole. It is conceivable that the proposed PV modifications are specific to *P. falciparum* where they may be necessary for the longevity of this compartment in the uniquely long gametocytogenesis of this parasite. In this respect, it is remarkable that of the 26 *PfGEXP* genes described here only four orthologs exist in the current gene annotation of rodent *Plasmodium* species (PB001016.01.0, PB000298.03.0, PB000716.00.0, and PB000835.03.0 in the case of *P. berghei*) in which gametocyte development is much faster, only slightly longer than the respective ~24-h asexual cycles. On the second issue, the limited available studies suggest that sequestration of the *P. falciparum* developing gametocytes in internal organs, chiefly the bone marrow and the spleen, relies on adhesive properties different from those of asexual parasites (2). Although late trophozoites and schizonts adhere to various endothelial cell types through interactions of the knob-located PfEMP1 molecules with host ligands, such as ICAM-1 and CD36, the mid-stage gametocytes do not have knobs (45), bind poorly to such ligands, and generally show a much lower affinity to endothelial cells also if of bone marrow origin (46).<sup>2</sup> Specific information on adhesive properties of early gametocytes is largely missing and partly controversial: one report showed that these stages show asexual-like adhesive properties and knobs (40), whereas the latter structures could not be detected in another study (45). In light of these observations, our data may suggest that the large use of gametocyte-enriched exported molecules may be at least in part functional in the yet undefined mechanisms of sexual-stage specific sequestration.

<sup>2</sup> F. Silvestrini, M. L. Tiburcio, L. Bertuccini, and P. Alano, unpublished results.

In conclusion, our work shows that at the onset of sexual differentiation the parasite specifically dedicates a relevant expression of its proteome to export proteins and to possibly modify the host erythrocyte with molecules enriched in this developmental stage. This observation and the genome-wide data produced here will be able to direct further work on these underexplored parasite stages and to unveil novel target mechanisms to interrupt gametocytogenesis in the frame of novel transmission-blocking strategies.

*Acknowledgments*—Prof. G. Girelli, University of Rome, and C. Currà and M. Ponzi, Istituto Superiore di Sanità, are acknowledged for the gifts of human red blood cells and for mouse immunization, respectively. Dr. P. Mortensen, Center for Experimental Bioinformatics, University of Southern Denmark, is acknowledged for help generating MS/MS spectra of single peptide hits.

\* This work was supported in part by European Union FP6 Network of Excellence Biology and Pathology of Malaria Parasite (BioMalPar) and by European Union FP7 Projects Signalling in Life Cycle Stages of Malaria Parasites (MALSIG) and European Virtual Institute for Malaria Research (EViMalaR).

§ This article contains supplemental Figs. S1–S5 and Tables S1–S5. § Both authors contributed equally to this work.

‡‡ Received partial support for the internship at Istituto Superiore di Sanità from Dr. A. Thomas and Dr. R. E. Bontrop, Biomedical Primate Research Centre, Rijswijk, The Netherlands.

§§ To whom correspondence should be addressed. Tel.: 39-064990-2868; Fax: 39-064990-2226; E-mail: alano@iss.it.

#### REFERENCES

- Hawking, F., Wilson, M. E., and Gammage, K. (1971) Evidence for cyclic development and short-lived maturity in the gametocytes of *Plasmodium falciparum*. *Trans. R. Soc. Trop. Med. Hyg.* **65**, 549–559
- Alano, P. (2007) *Plasmodium falciparum* gametocytes: still many secrets of a hidden life. *Mol. Microbiol.* **66**, 291–302
- Bruce, M. C., Carter, R. N., Nakamura, K., Aikawa, M., and Carter, R. (1994) Cellular location and temporal expression of the *Plasmodium falciparum* sexual stage antigen Pfs16. *Mol. Biochem. Parasitol.* **65**, 11–22
- Carter, R., Graves, P. M., Creasey, A., Byrne, K., Read, D., Alano, P., and Fenton, B. (1989) *Plasmodium falciparum*: an abundant stage-specific protein expressed during early gametocyte development. *Exp. Parasitol.* **69**, 140–149
- Silvestrini, F., Bozdech, Z., Lanfrancotti, A., Di Giulio, E., Bultrini, E., Picci, L., Derisi, J. L., Pizzi, E., and Alano, P. (2005) Genome-wide identification of genes upregulated at the onset of gametocytogenesis in *Plasmodium falciparum*. *Mol. Biochem. Parasitol.* **143**, 100–110
- Eksi, S., Haile, Y., Furuya, T., Ma, L., Su, X., and Williamson, K. C. (2005) Identification of a subtelomeric gene family expressed during the asexual-sexual stage transition in *Plasmodium falciparum*. *Mol. Biochem. Parasitol.* **143**, 90–99
- Furuya, T., Mu, J., Hayton, K., Liu, A., Duan, J., Nkrumah, L., Joy, D. A., Fidock, D. A., Fujioka, H., Vaidya, A. B., Welles, T. E., and Su, X. Z. (2005) Disruption of a *Plasmodium falciparum* gene linked to male sexual development causes early arrest in gametocytogenesis. *Proc. Natl. Acad. Sci. U.S.A.* **102**, 16813–16818
- Young, J. A., Fivelman, Q. L., Blair, P. L., de la Vega, P., Le Roch, K. G., Zhou, Y., Carucci, D. J., Baker, D. A., and Winzeler, E. A. (2005) The *Plasmodium falciparum* sexual development transcriptome: a microarray analysis using ontology-based pattern identification. *Mol. Biochem. Parasitol.* **143**, 67–79
- Lasonder, E., Ishihama, Y., Andersen, J. S., Vermunt, A. M., Pain, A., Sauerwein, R. W., Eling, W. M., Hall, N., Waters, A. P., Stunnenberg, H. G., and Mann, M. (2002) Analysis of the *Plasmodium falciparum* proteome by high-accuracy mass spectrometry. *Nature* **419**, 537–542
- Florens, L., Washburn, M. P., Raine, J. D., Anthony, R. M., Grainger M.,

- Haynes, J. D., Moch, J. K., Muster, N., Sacchi, J. B., Tabb, D. L., Witney, A. A., Wolters, D., Wu, Y., Gardner, M. J., Holder, A. A., Sinden, R. E., Yates, J. R., and Carucci, D. J. (2002) A proteomic view of the *Plasmodium falciparum* life cycle. *Nature* **419**, 520–526
11. Khan, S. M., Franke-Fayard, B., Mair, G. R., Lasonder, E., Janse, C. J., Mann, M., and Waters, A. P. (2005) Proteome analysis of separated male and female gametocytes reveals novel sex-specific *Plasmodium* biology. *Cell* **121**, 675–687
12. Subramanian, A., Tamayo, P., Mootha, V. K., Mukherjee, S., Ebert, B. L., Gillette, M. A., Paulovich, A., Pomeroy, S. L., Golub, T. R., Lander, E. S., and Mesirov, J. P. (2005) Gene set enrichment analysis: a knowledge-based approach for interpreting genome-wide expression profiles. *Proc. Natl. Acad. Sci. U.S.A.* **102**, 15545–15550
13. Ishihama, Y., Oda, Y., Tabata, T., Sato, T., Nagasu, T., Rappsilber, J., and Mann, M. (2005) Exponentially modified protein abundance index (emPAI) for estimation of absolute protein amount in proteomics by the number of sequenced peptides per protein. *Mol. Cell. Proteomics* **4**, 1265–1272
14. Walliker, D., Quakyi, I. A., Wellems, T. E., McCutchan, T. F., Szarfman, A., London, W. T., Corcoran, L. M., Burkot, T. R., and Carter, R. (1987) Genetic analysis of the human malaria parasite *Plasmodium falciparum*. *Science* **236**, 1661–1666
15. Alano, P., Roca, L., Smith, D., Read, D., Carter, R., and Day, K. (1995) *Plasmodium falciparum*: parasites defective in early stages of gametocytogenesis. *Exp. Parasitol.* **81**, 227–235
16. Olivieri, A., Silvestrini, F., Sanchez, M., and Alano, P. (2008) A 140-bp AT-rich sequence mediates positive and negative transcriptional control of a *Plasmodium falciparum* developmentally regulated promoter. *Int. J. Parasitol.* **38**, 299–312
17. O'Donnell, R. A., Freitas-Junior, L. H., Preiser, P. R., Williamson, D. H., Duraisingh, M., McElwain, T. F., Scherf, A., Cowman, A. F., and Crabb, B. S. (2002) A genetic screen for improved plasmid segregation reveals a role for Rep20 in the interaction of *Plasmodium falciparum* chromosomes. *EMBO J.* **21**, 1231–1239
18. Ifediba, T., and Vanderberg, J. P. (1981) Complete in vitro maturation of *Plasmodium falciparum* gametocytes. *Nature* **294**, 364–366
19. Rappsilber, J., Ishihama, Y., and Mann, M. (2003) Stop and go extraction tips formatix-assisted laser desorption/ionization, nanoelectrospray, and LC/MS sample pretreatment in proteomics. *Anal. Chem.* **75**, 663–670
20. Cox, J., and Mann, M. (2008) MaxQuant enables high peptide identification rates, individualized p.p.b.-range mass accuracies and proteome-wide protein quantification. *Nat. Biotechnol.* **26**, 1367–1372
21. Lasonder, E., Janse, C. J., van Gemert, G. J., Mair, G. R., Vermunt, A. M., Douradinha, B. G., van Noort, V., Huynen, M. A., Luty, A. J., Kroeze, H., Khan, S. M., Sauerwein, R. W., Waters, A. P., Mann, M., and Stunnenberg, H. G. (2008) Proteomic profiling of *Plasmodium* sporozoite maturation identifies new proteins essential for parasite development and infectivity. *PLoS Pathog.* **4**, e1000195
22. Saeed, A. I., Sharov, V., White, J., Li, J., Liang, W., Bhagabati, N., Braisted, J., Klapa, M., Currier, T., Thiagarajan, M., Sturn, A., Snuffin, M., Rezantsev, A., Popov, D., Ryltsov, A., Kostukovich, E., Borisovsky, I., Liu, Z., Vinsavich, A., Trush, V., and Quackenbush, J. (2003) TM4: a free, open-source system for microarray data management and analysis. *BioTechniques* **34**, 374–378
23. Zhou, Y., Young, J. A., Santosyan, A., Chen, K., Yan, S. F., and Winzeler, E. A. (2005) In silico gene function prediction using ontology-based pattern identification. *Bioinformatics* **21**, 1237–1245
24. Sargeant, T. J., Marti, M., Caler, E., Carlton, J. M., Simpson, K., Speed, T. P., and Cowman, A. F. (2006) Lineage-specific expansion of proteins exported to erythrocytes in malaria parasites. *Genome Biol.* **7**, R12
25. Marti, M., Good, R. T., Rug, M., Knuepfer, E., and Cowman, A. F. (2004) Targeting malaria virulence and remodeling proteins to the host erythrocyte. *Science* **306**, 1930–1933
26. Hiss, J. A., Przyborski, J. M., Schwarte, F., Lingelbach, K., and Schneider, G. (2008) The *Plasmodium* export element revisited. *PLoS One* **3**, e1560
27. Olsen, J. V., Blagoev, B., Gnäd, F., Macek, B., Kumar, C., Mortensen, P., and Mann, M. (2006) Global, in vivo, and site-specific phosphorylation dynamics in signaling networks. *Cell* **127**, 635–648
28. Chang, H. H., Falick, A. M., Carlton, P. M., Sedat, J. W., DeRisi, J. L., and Marletta, M. A. (2008) N-terminal processing of proteins exported by malaria parasites. *Mol. Biochem. Parasitol.* **160**, 107–115
29. Tonkin, C. J., van Dooren, G. G., Spurck, T. P., Struck, N. S., Good, R. T., Handman, E., Cowman, A. F., and McFadden, G. I. (2004) Localization of organellar proteins in *Plasmodium falciparum* using a novel set of transfection vectors and a new immunofluorescence fixation method. *Mol. Biochem. Parasitol.* **137**, 13–21
30. Gupta, S. K., Schulman, S., and Vanderberg, J. P. (1985) Stage-dependent toxicity of N-acetyl-glucosamine to *Plasmodium falciparum*. *J. Protozool.* **32**, 91–95
31. de Koning-Ward, T. F., Olivieri, A., Bertuccini, L., Hood, A., Silvestrini, F., Charvalias, K., Berzosa Díaz, P., Camarda, G., McElwain, T. F., Papenfuss, T., Healer, J., Baldassarri, L., Crabb, B. S., Alano, P., and Ranford-Cartwright, L. C. (2008) The role of osmiophilic bodies and Pfg377 expression in female gametocyte emergence and mosquito infectivity in the human malaria parasite *Plasmodium falciparum*. *Mol. Microbiol.* **67**, 278–290
32. Eksi, S., and Williamson, K. C. (2002) Male-specific expression of the paralog of malaria transmission-blocking target antigen Pfs230, PfB0400w. *Mol. Biochem. Parasitol.* **122**, 127–130
33. Kaslow, D. C., Quakyi, I. A., Syin, C., Raum, M. G., Keister, D. B., Coligan, J. E., McCutchan, T. F., and Miller, L. H. (1988) A vaccine candidate from the sexual stage of human malaria that contains EGF-like domains. *Nature* **333**, 74–76
34. Rawlings, D. J., Fujioka, H., Fried, M., Keister, D. B., Aikawa, M., and Kaslow, D. C. (1992) Alpha-tubulin II is a male-specific protein in *Plasmodium falciparum*. *Mol. Biochem. Parasitol.* **56**, 239–250
35. Vermeulen, A. N., van Deursen, J., Brakenhoff, R. H., Lensen, T. H., Ponudurai, T., and Meuwissen, J. H. (1986) Characterization of *Plasmodium falciparum* sexual stage antigens and their biosynthesis in synchronised gametocyte cultures. *Mol. Biochem. Parasitol.* **20**, 155–163
36. Dixon, M. W., Thompson, J., Gardiner, D. L., and Trenholme, K. R. (2008) Sex in *Plasmodium*: a sign of commitment. *Trends Parasitol.* **24**, 168–175
37. Spielmann, T., Hawthorne, P. L., Dixon, M. W., Hannemann, M., Klotz, K., Kemp, D. J., Klönis, N., Tilley, L., Trenholme, K. R., and Gardiner, D. L. (2006) A cluster of ring stage-specific genes linked to a locus implicated in cytoadherence in *Plasmodium falciparum* codes for PEXEL-negative and PEXEL-positive proteins exported into the host cell. *Mol. Biol. Cell* **17**, 3613–3624
38. Botha, M., Pesce, E. R., and Blatch, G. L. (2007) The Hsp40 proteins of *Plasmodium falciparum* and other apicomplexa: regulating chaperone power in the parasite and the host. *Int. J. Biochem. Cell Biol.* **39**, 1781–1803
39. Maier, A. G., Rug, M., O'Neill, M. T., Brown, M., Chakravorty, S., Szestak, T., Chesson, J., Wu, Y., Hughes, K., Coppel, R. L., Newbold, C., Beeson, J. G., Craig, A., Crabb, B. S., and Cowman, A. F. (2008) Exported proteins required for virulence and rigidity of *Plasmodium falciparum*-infected human erythrocytes. *Cell* **134**, 48–61
40. Day, K. P., Hayward, R. E., Smith, D., and Culvenor, J. G. (1998) CD36-dependent adhesion and knob expression of the transmission stages of *Plasmodium falciparum* is stage specific. *Mol. Biochem. Parasitol.* **93**, 167–177
41. Boddey, J. A., Hodder, A. N., Günther, S., Gilson, P. R., Patsiouras, H., Kapp, E. A., Pearce, J. A., de Koning-Ward, T. F., Simpson, R. J., Crabb, B. S., and Cowman, A. F. (2010) An aspartyl protease directs malaria effector proteins to the host cell. *Nature* **463**, 627–631
42. Russo, I., Babbitt, S., Muralidharan, V., Butler, T., Oksman, A., and Goldberg, D. E. (2010) Plasmeprin V licenses *Plasmodium* proteins for export into the host erythrocyte. *Nature* **463**, 632–636
43. de Koning-Ward, T. F., Gilson, P. R., Boddey, J. A., Rug, M., Smith, B. J., Papenfuss, A. T., Sanders, P. R., Lundie, R. J., Maier, A. G., Cowman, A. F., and Crabb, B. S. (2009) A newly discovered protein export machine in malaria parasites. *Nature* **459**, 945–949
44. Boddey, J. A., Moritz, R. L., Simpson, R. J., and Cowman, A. F. (2009) Role of the *Plasmodium* export element in trafficking parasite proteins to the infected erythrocyte. *Traffic* **10**, 285–299
45. Sinden, R. E. (1982) Gametocytogenesis of *Plasmodium falciparum* in vitro: an electron microscopic study. *Parasitology* **84**, 1–11
46. Rogers, N. J., Hall, B. S., Obiero, J., Targett, G. A., and Sutherland, C. J. (2000) A model for sequestration of the transmission stages of *Plasmodium falciparum*: adhesion of gametocyte-infected erythrocytes to human bone marrow cells. *Infect. Immun.* **68**, 3455–3462